

**APPLICATION OF A RATIOMETRIC LASER INDUCED FLUORESCENCE
(LIF) THERMOMETRY FOR MICRO-SCALE TEMPERATURE
MEASUREMENT FOR NATURAL CONVECTION FLOWS**

A Thesis

by

HEON JU LEE

Submitted to the Office of Graduate Studies of
Texas A&M University
in partial fulfillment of the requirements for the degree of

MASTER OF SCIENCE

August 2003

Major Subject: Mechanical Engineering

**APPLICATION OF A RATIOMETRIC LASER INDUCED FLUORESCENCE
(LIF) THERMOMETRY FOR MICRO-SCALE TEMPERATURE
MEASUREMENT FOR NATURAL CONVECTION FLOWS**

A Thesis

by

HEON JU LEE

Submitted to the Office of Graduate Studies of
Texas A&M University
in partial fulfillment of the requirements for the degree of

MASTER OF SCIENCE

Approved as to style and content by:

Kenneth D. Kihm
(Chair of Committee)

Sai Lau
(Member)

James Boyd
(Member)

Dennis O'Neal
(Interim Head of Department)

August 2003

Major Subject: Mechanical Engineering

ABSTRACT

Application of a Ratiometric Laser Induced Fluorescence (LIF) Thermometry
for Micro-scale Temperature Measurement for Natural Convection Flows.

(August 2003)

Heon Ju Lee, B.S., Korea University, Korea

Chair of Advisory Committee: Dr. Kenneth D. Kihm

A ratiometric laser induced fluorescence (LIF) thermometry applied to micro-scale temperature measurement for natural convection flows. To eliminate incident light non-uniformity and imperfection of recording device, two fluorescence dyes are used: one is temperature sensitive fluorescence dye (Rhodamine B) and another is relatively temperature insensitive fluorescence dye (Rhodamine 110). Accurate and elaborate calibration for intensity ratio versus temperature obtained using an isothermal cuvette, which was controlled by two thermo-bathes. 488nm Ar-ion laser used for incident light and two filter sets used for separating each fluorescence emission.

Thermally stratified fluid of 10mm channel with micro-scale resolution measured within 1.3°C uncertainty of linear prediction with 23 μ m x 23 μ m spatial resolution. Natural convection flows at 10mm channel also observed.

The several difficulties for applying to heated evaporating meniscus were identified and a few resolutions were suggested.

ACKNOWLEDGEMENTS

I would like to express my sincere gratitude to my advisor, Dr. Kenneth D. Kihm, for his support guidance and contributions in all aspects of the research and for encouragement to keep engineering mind. I'll always keep that in my mind on my future research. Special thanks also go to Dr. Sai Lau and Dr. James Boyd for their time and effort to assist me in the completion of this research.

Appreciation goes to all the colleagues in Dr. Kihm's laboratory for their friendship and assistance during the past two years of my graduate education.

Most of all, the deepest appreciation goes to my family, specially for parents, Chung Cha Kim and Chun Sik Lee, for their encouragement and support throughout my life, and I'll never forget the financial support from my lovely sisters. This work would not have been completed without their deepest care and love.

Thanks also to my girlfriend, Hyun Zoo, for her patience and encouragement throughout the duration of my study.

TABLE OF CONTENTS

	Page
ABSTRACT.....	iii
ACKNOWLEDGEMENTS.....	vi
TABLE OF CONTENTS.....	v
LIST OF FIGURES.....	vii
LIST OF TABLES.....	ix
NOMENCLATURE	x
 CHAPTER	
I INTRODUCTION.....	1
1.1 Literature Review.....	1
1.2 Summary of Present Study.....	2
II BACKGROUND.....	4
2.1 Principle of Fluorescence & Ratiometric LIF Techniques	4
2.2 Spectral Characteristics of Rhodamine 110 and Rhodamine B.....	8
III EXPERIMENTATION AND RESULTS.....	10
3.1 Calibration Process and Results.....	10
3.2 Temperature Measurement for Thermally Stratified Fields.....	16
3.3 Temperature Measurement for Natural Convection Fields.....	21
IV DISCUSSION.....	24
4.1 Difficulties for Temperature Measurement for Heated Evaporating Meniscus.....	24
4.2 Suggestion of a Remedy for Intensity Bias.....	27
V CONCLUSION.....	30

CHAPTER	Page
VI RECOMMENDATIONS FOR FUTURE STUDY.....	31
REFERENCES.....	32
VITA.....	34

LIST OF FIGURES

FIGURE	Page
2.1	The Creation of an Excited Electronic Single State by Optical Absorption and Subsequent Emission of Fluorescence..... 4
2.2	Spectral Characteristics of Rhodamine 110 and Rhodamine B: Their Absorption and Emission Wavelengths (Molecular Probes)..... 8
2.3	Incident Laser Wavelength (488nm) and Filtering System: (Bandpass Filter for 510nm and Longpass Filter for Larger than 560nm)..... 9
3.1	Experimental Setup for Calibration Process: The White Arrows Represent That Water Circulates the Thermo-baths to Maintain Isothermal Conditions.. 10
3.2	Temperature Dependence of Fluorescence Images of Rh-B (column (a)), Rh-110 (column (b)) and Their Ratiometric Images (column (c))..... 12
3.3	Pixel Averaged Intensity of Rh-B and RH-110 Emission vs Temperature.... 13
3.4	Intensity Ratio vs Temperature..... 14
3.5	Intensity Ratio vs Temperature: Derivation of Intensity with Interrogation Window Size..... 15
3.6	Thermally Stratified Fields with Three Different Conditions..... 17
3.7	Line-averaged Measurement Result with Linear Prediction for Top 29°C and Bottom 24°C..... 18
3.8	Line-averaged Measurement Result with Linear Prediction for Top 34°C and Bottom 24°C..... 19
3.9	Line-averaged Measurement Result with Linear Prediction for Top 39°C and Bottom 24°C..... 20
3.10	Natural Convection Flows with Three Different Conditions 22

FIGURE	Page
4.1 Test Section for Heated Evaporating Meniscus.....	25
4.2 Raw Images of Meniscus at 21.6°C.....	26
4.3 Ratiometric LIF Result with Previous Calibration Data at Meniscus Region	26
4.4 Error Terms Coming from Internal Reflection: Re-absorption and Direct Detection.....	27
4.5 Result after Second Calibration the Top T/C Reading is 38°C and Bottom T/C Reading is 22.5°C.....	29
4.6 Compensation Factor (a) and Lens Effect (b).....	29

LIST OF TABLES

TABLE	Page
3.1 Spatial Resolution and Corresponding Temperature Deviation for Calibration Data.....	14
3.2 Standard Derivation of Temperature for Linear Prediction with Interrogation Window Size.....	21

NOMENCLATURE

$[c]$	Concentration
F	Fluorescence Intensity
I	Intensity
Q	Quantum efficiency
T	Temperature
L	Length
t	Time
τ	Excited state life time
ε	Molecular Absorptivity
β	Thermal coefficient of volume expansion
λ	Laser light wave length
ν	Kinematic Viscosity
Ra	Raleigh number
Pr	Prandtl number
Gr	Grashof number

CHAPTER I

INTRODUCTION

Chapter I presents general introduction to the application, background and purpose of this research. Section 1.1 provides literature review. In Section 1.2, a summary of research contents is presented.

1.1 LITERATURE REVIEW

Micro-scale fluidics and heat transfer phenomena has been studied for developing micro devices at MEMS (Micro-Electronic-Mechanical Systems) and for performing micro-gravity experiments for modeling space environment.

For fluid flows in micro-scale, a Lagrangian velocity mapping technique using a caged fluorescence dye (MTFV: Molecular Tagging Fluorescence Velocimetry) and full field velocity measurement technique, which is using a confocal microscope system (micro- PIV) have been developed ([1]). However, for temperature measurement in micro-scale was not easy to approach, because of limitation of spatial resolution of exist temperature measurement techniques. Applying optical method, LIF (Laser Induced

Fluorescence) technique had been developed using the temperature sensitive fluorescence dye to measure the temperature ([2]). However, this technique is very difficult to ensure a homogeneous incident light intensity distribution and the imperfection of recording means can hardly guarantee persistent intensity levels even under uniform lighting and constant dye concentration. To overcome this problem, an innovative two-color LIF technique proposed ([3], [4]). They used a second temperature-insensitive fluorescence dye (Rhodamine-110) as a reference to compensate for the variation of incident light and the spatial imaging nonuniformity. The ratio of the two fluorescent intensities provides a formidable correlation with temperature that does not depend on the laser illumination intensity variation and is free from the possible bias occurring from background noise. This Two-color LIF technique applied for micro channel to measure the temperature and obtained spatial resolution of $300\mu\text{m}$ by $200\mu\text{m}$ at ± 1.5 °C temperature uncertainty with 95% confidence at 10mm and 1mm micro channel ([5]).

1.2 SUMMARY OF PRESENT STUDY

The objective of the proposed research is the application of Two-Color Laser Induced Fluorescence Technique ([3]. [4] and [5]) for temperature measurement in micro-scale.

Temperature is the most essential property to examine heat transport phenomena. Though existing temperature measurement techniques are quite reliable within $\pm 0.1\text{K}$ precision, but it has relatively large spatial resolution on the order of

hundred microns. However one of the most efficient heat transfer phenomena, evaporation, occurs on the order of from hundred nanometer to hundred of micrometer ([6], [7]). There is no other method that can provide such a small spatial resolution but two-color LIF technique. Not only in the thin film evaporating phenomena but also in micro-gravity experiments this technique make it possible to measure full field temperature profiles. Proposed experiments focus on developing this technique.

In this study, accurate and elaborate calibration for intensity ratio verses temperature obtained using an isothermal cuvette, which was controlled by two thermostats. To ensure this calibration data, thermally stratified temperature field at 10mm channel was measured and compared with T/C's (thermo-couples) reading which are attached between channel wall and thermal reservoir. Natural convection was measured with micro-scale resolution in 10mm channel and isothermal contour was obtained for circulating flow.

In the area of heated evaporating meniscus, there is intensity bias occurring from the internal reflection from the curvature of meniscus. In this study, the problems to apply ratiometric LIF Thermometry at heated evaporating meniscus was identified and several solutions to alleviate this intensity bias was suggested.

CHAPTER II

BACKGROUND

2.1 PRINCIPLE OF FLUORESCENCE & RATIOMETRIC LIF TECHNIQUES

Fluorescence is the property of an atom or a molecule that is excited by incident light at a particular wavelength to a stimulated absorption state at a higher quantum energy level, and after a very short interval, termed the fluorescence lifetime, re-emits light at longer wavelengths in Fig. 2.1. The absorption of a photon of energy by

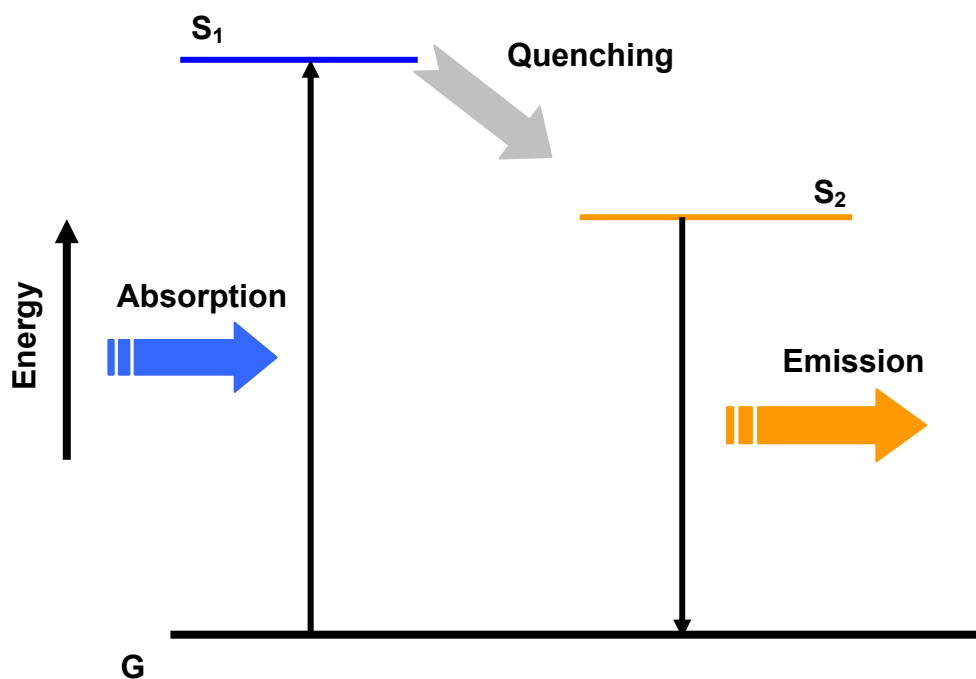


Fig. 2.1 The Creation of an Excited Electronic Single State by Optical Absorption and Subsequent Emission of Fluorescence

fluorescent molecule can only absorb incident light of certain specific wavelength known as absorption band. Emission of fluorescence also occurs at certain specific wavelength, but this wavelength is at lower energy-longer wavelength value-than absorption band maximum (the Stokes' Law) due to loss of energy by the molecules during interactions with its environment before it emits its fluorescence (internal conversion). Absorption of energy by fluorescent molecules occurs between a number of closely spaced vibrational and rotational excited states in different orbital. Physically, absorption of light occurs in very short period (approximately 10^{-15} second) and corresponds to the excitation of the fluorophore from the ground state to an excited state. Relaxation to the lowest excited singlet state, known as internal conversion, occurs within approximately 10^{-11} second as energy is thermally transferred to the environment. Internal conversion (loss of energy in the absence of emission of light) is due to collision of the excited state probe with solvent molecules. The molecule lives in the lowest excited singlet state for periods of the order of nanoseconds (approximately 10^{-9} second). Relaxation from this state (the lowest excited singlet, S_2) in Fig. 2.1 to the ground state with emission of a photon is, physically, what is referred to as fluorescence.

Fluorescence intensity at a specified point is expressed as ([8]):

$$F = I_0 \varepsilon [c] Q \quad (2.1)$$

where F is the measured fluorescence intensity for a fluorescent dye with molar absorptivity of ε at a point in the incident light with intensity I_0 , with the fluorescence dye concentration $[c]$, and the quantum efficiency Q . The quantum

yield, Q is a measure of the emission efficiency of the fluorophore and is expressed as the ratio of photons emitted to photons absorbed.

$$Q = \frac{\textit{photons emitted}}{\textit{photons absorbed}} \quad (2.2)$$

The value of absorptivity, ϵ is usually expressed at the maximum wavelength of absorption, while Q is a measure of the total photon emission over the entire fluorescence spectrum. Thus, the amount of fluorescence is proportional to the product of the light absorbed by the fluorophore and the quantum efficiency Q . Fluorescent molecules that absorb energy move from ground state (G) to the excited state (S_1), as schematically illustrated in Fig. 2.1. The quenching effect makes relaxation or non-radiative emission to the lower excited state (S_2), decreasing the quantum efficiency Q to less than unity. Since these effects occur without emission of photon, they are termed quenching. For example, collision of the excited fluorophore with another molecule resulting in non radiative transfer of the excited state energy to this molecule is termed internal conversion or collisional or dynamic quenching. Dynamic fluorescence quenching can reflect the presence of proximate quencher molecules or groups which, via diffusion or conformational exchange, may collide with the fluorophore during the excited state lifetime. Such quenching acts to reduce the excited state lifetime, τ , and the quantum efficiency, Q . Due to this quenching the quantum efficiency is always less than 1. As the temperature increases, the quenching effect increases and the quantum efficiency decreases. The temperature dependence of quantum efficiency is usually small

in most fluorescent molecules. However, for some fluorescence dyes such as Rhodamine-B, the temperature dependence of quantum efficiency is noticeably high, about 2%/K. As mentioned previously, fluorescent light intensity is proportional to the incident light intensity. Incident light is likely to be inhomogeneous, spatially as well as temporally, because of the laser beam or sheet divergence, scattering by small particles in the beam path, and time-dependent lasting efficiency ([4], [5]). In order to compensate the measurement bias caused by the incident light variation, Rhodamine-110 is used for the reference dye whose photo-thermal sensitivity is known to be less than 0.05%/K.

For the mixture of Rhodamine-B and Rhodamine-110, the intensity ratio of the two fluorescence emissions can be directly given from Eq. (2.1) as:

$$\frac{F_{rhh}}{F_{rh110}} = \frac{I_{0rhh} \varepsilon_{rhh} [c]_{rhh} Q_{rhh}}{I_{0rh110} \varepsilon_{rh110} [c]_{rh110} Q_{rh110}} \quad (2.3)$$

where molar absorptivity ε is nearly independent of temperature ([9]), and the ratio of the absorption spectral intensity, I_{0rhh} / I_{0rh110} , is invariant when a single illumination source is used for both dyes. In addition, if the concentration ratio, $[c]_{rhh} / [c]_{rh110}$, remains unchanged, the fluorescence intensity ratio, F_{rhh} / F_{rh110} , is solely dependent on the quantum efficiency ratio of the two dyes, Q_{rhh} / Q_{rh110} . Since the ratio of the quantum efficiency depends on temperature, the resulting intensity ratio of Eq. (2.3) can now be considered solely dependent on temperature.

2.2 SPECTRAL CHARACTERISTICS OF RHODAMINE 110 AND RHODAMINE B

Figure 2.2 shows the semi-quantitative absorption and emission spectra of Rhodamine-B and Rhodamine-110. The wavelength of maximum absorption and emission for Rhodamine-110 (Molecular Probes) is at 496-nm and 520-nm, respectively. Rhodamine-B (J. T. Baker, Inc.) has an absorption band peaked at 554-nm and an emission band peaked at 575-nm. These four bandwidths partially overlap each other. To minimize signal errors due to the cross-talk, the fluorescence detection band for each dye must be segregated from the other emission and absorption bandwidths, to the extent possible. For the Rhodamine-B detection bands, selection is made for the long pass filter

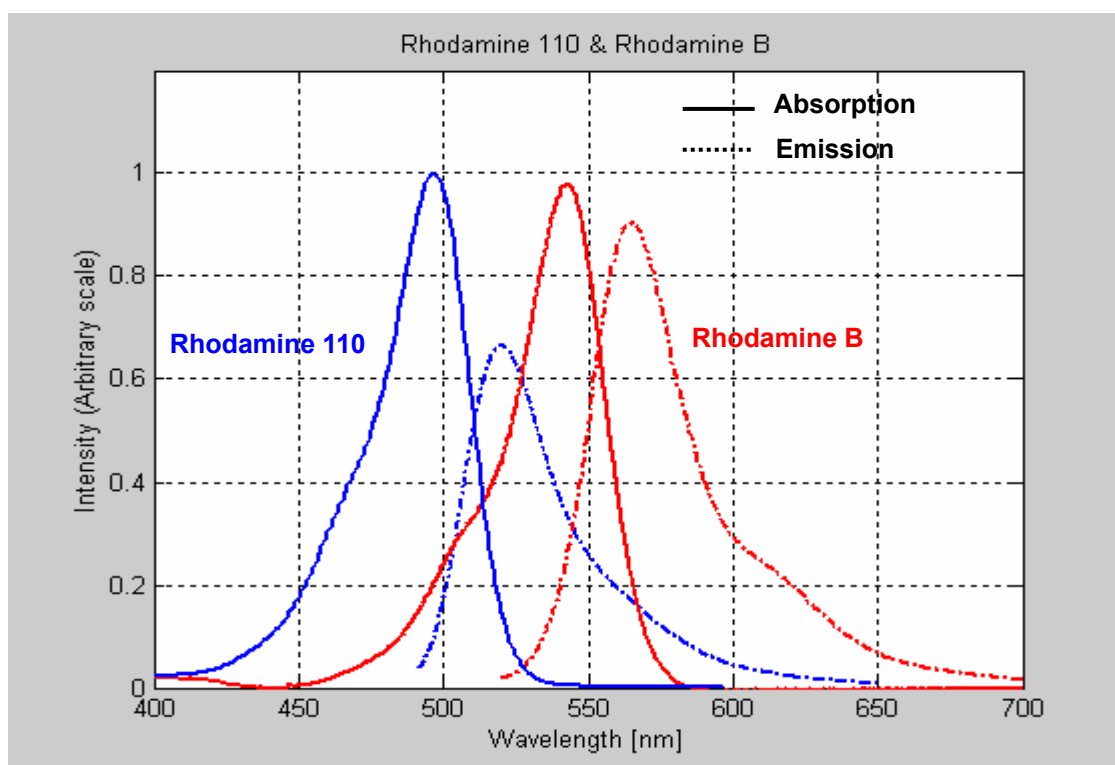


Fig. 2.2 Spectral Characteristics of Rhodamine 110 and Rhodamine B: Their Absorption and Emission Wavelengths (Molecular Probes)

(Edmund Industrial Optics) that transmits wavelengths only longer than 560-nm. This filter has a mere 0.001% transmission of shorter wavelengths than 560-nm. Since Rhodamine-110 emission band is placed between the Rh-110 absorption band and Rh-B absorption band, a narrow band-pass filter (505-nm ~ 515-nm) is selected to effectively separate the Rh-110 emissions. The spectral band of an argon-ion laser, peaked at 488-nm (blue), is used to excite both dyes. Figure 2.3 Shows incident laser wavelength and filters with fluorescence absorption and emission spectra.

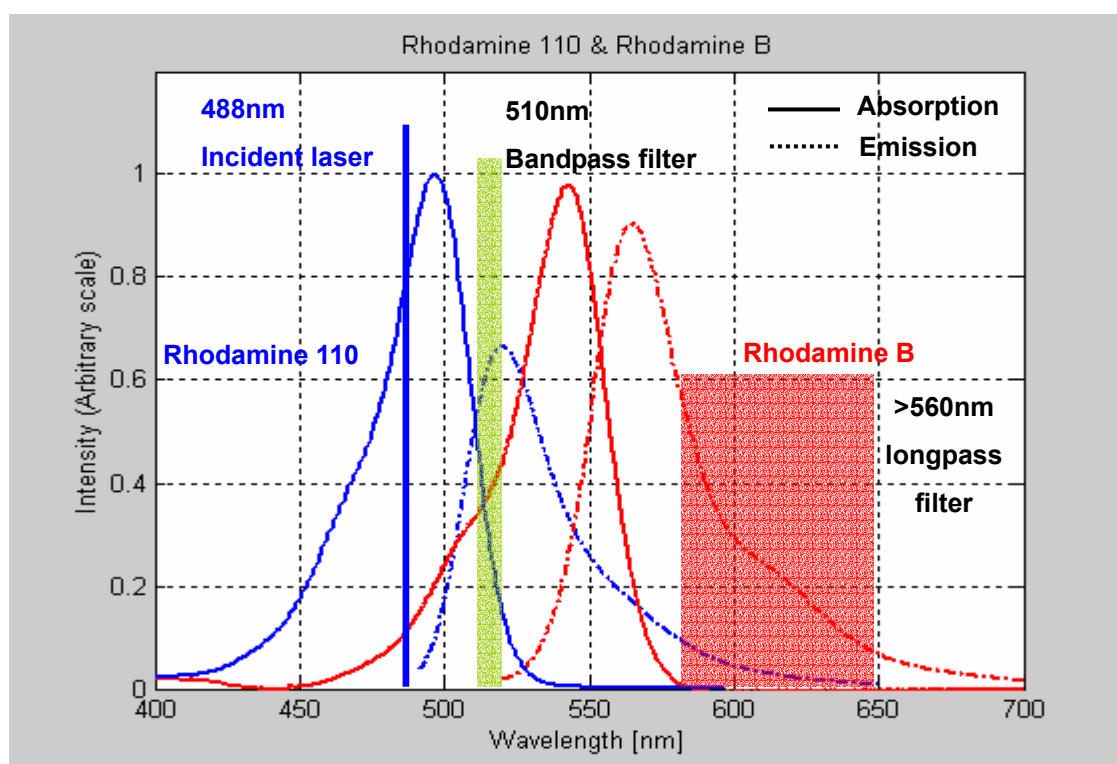


Fig 2.3 Incident Laser Wavelength (488nm) and Filtering System: (Bandpass Filter for 510nm and Longpass Filter for Larger than 560nm)

CHAPTER III

EXPERIMENTATION AND RESULTS

3.1 CALIBRATION PROCESS AND RESULTS

The correlation between the ratio of fluorescence intensities and temperature is necessary to use a LIF technique for temperature measurement. To obtain a correlation between the measured fluorescence intensity and the water temperature, an elaborate calibration system is devised. As schematically illustrated in Fig. 3.1, the apparatus consisted with a couple of accurately controlled thermo-baths, thermo-couples for continuously sensing the temperature, series of lens sets for obtaining thin laser sheet and test cuvette. The water circulates thermo-baths with constant-temperature at every set and the heat from the water transferred to copper plates to maintain isothermal

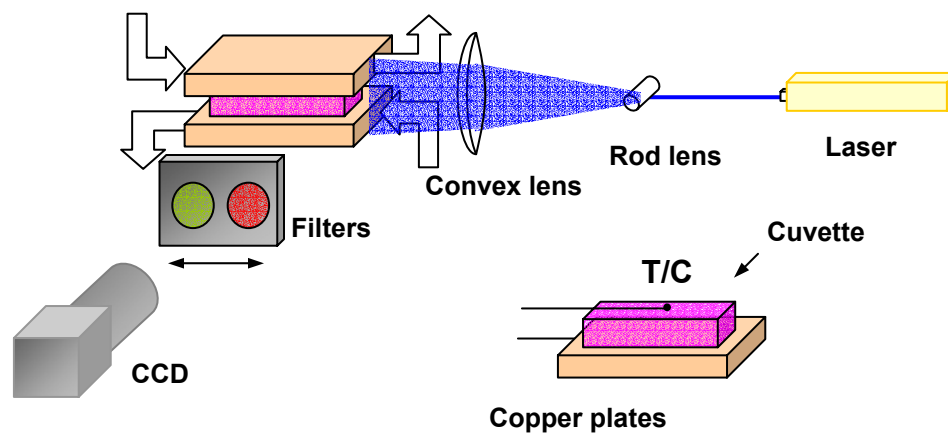


Fig. 3.1 Experimental Setup for Calibration Process: The White Arrows Represent That Water Circulates Thermo-Baths to Maintain Isothermal Conditions

condition. The test cuvette (Cole Parmer) contains Di-water with a 6mg/liter concentration of Rh-B and 1mg/liter concentration of Rh-110, and the cuvette is

squeezed between two copper plates which have 10mm thickness. The solution temperature filled in the cuvette was monitored using each thermocouple probes placed between copper plate and cuvette wall. A Sony XC-75 CCD camera records fluorescence images from Rh-B and Rh-110 by alternating the two filters and an approximately 8mm by 6mm field-of-view is used for calibration, corresponding to 640 x 480 pixel dimensions. A thin laser sheet, approximately 250 μ m, is constructed from a 50-mW argon-ion laser using a combination of one concave lens and one rod lens. Captured images from the CCD camera are digitized for successive gray-level analysis.

The column (a) of Fig. 3.2 shows a series of fluorescence images (8mm by 6mm field-of-view) taken for Rh-B for four different bath temperatures, the column (b) shows corresponding images for Rh-110, and the column (c) presents the ratio of the two images, the former to the latter. The Rh-B images clearly show the temperature dependence of the intensity that decreases with increasing temperatures whereas Rh-110 images are nearly invariant with temperature increases. The background intensity variations, due to laser incident direction, right side is brighter than left side, cause laser beam comes from left side. However, when the Rh-B images are normalized by the corresponding Rh-110 images, the background variations are cancelled out and the resulting ratio images are highly homogeneous. It shows a monotonic decrease with increasing temperature.

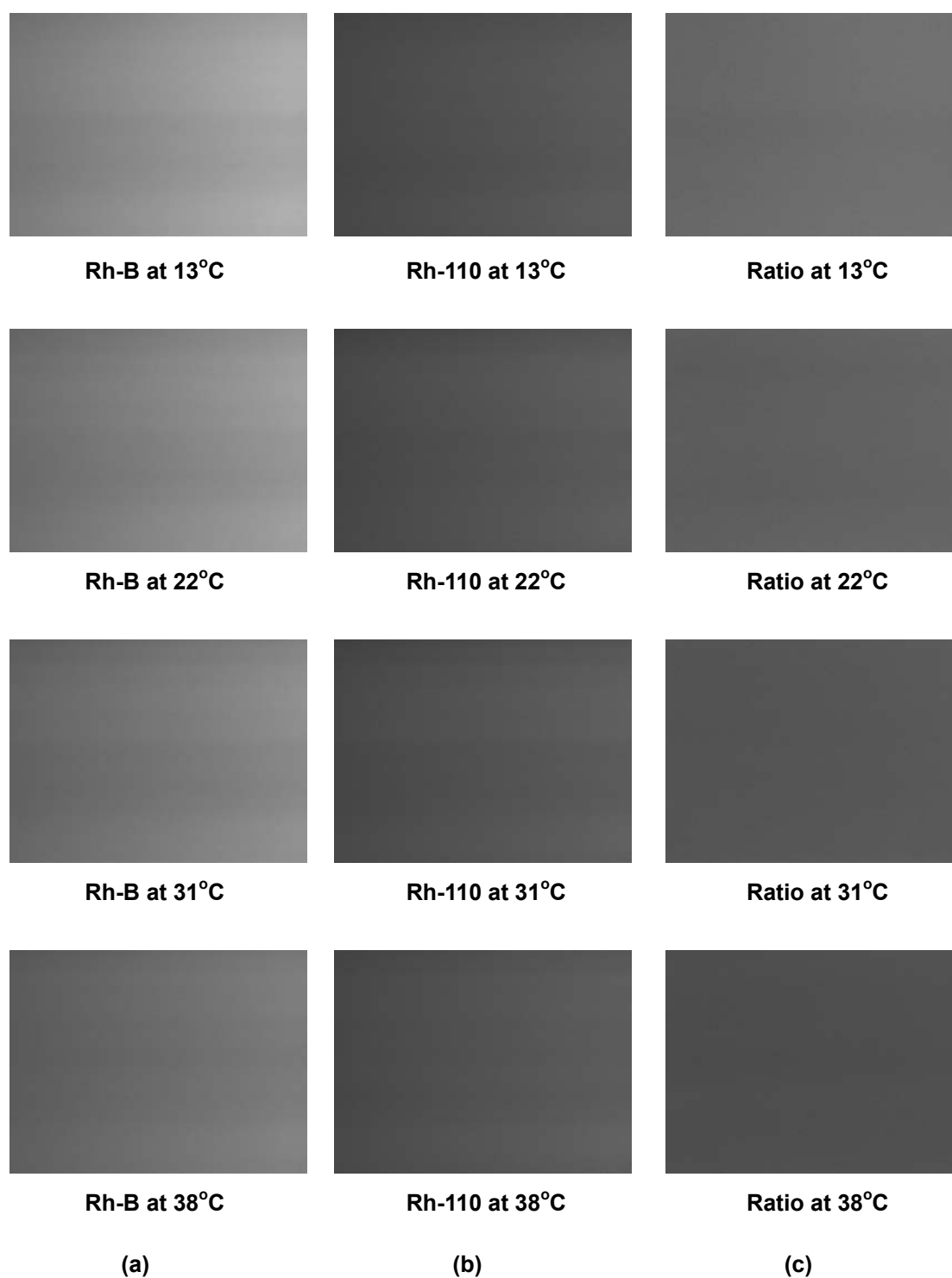


Fig. 3.2 Temperature Dependence of Fluorescence Images of Rh-B (column (a)), Rh-110 (column (b)) and Their Ratiometric Images (column (c))

The temperature range from 13°C to 38°C . Fig. 3.3 shows measured intensity variations for the two dyes and Fig. 3.4 shows intensity ratio verse temperature. Each symbol represents a pixel-averaged intensity for the entire 8mm x 6mm field-of-view (640 by 480 pixels). The fluorescence intensity of Rh-B decreases with increasing temperature while the fluorescence intensity of Rh-110 remains nearly constant.

Fig. 3.3 and Fig. 3.4 are based on the smallest spatial resolution of a single pixel, that is equivalent to a spatial resolution of about $12.5\ \mu\text{m}$ by $12.5\ \mu\text{m}$. To examine the effect of spatial resolution on the intensity variations, statistical analysis of the calibration data has been conducted as the interrogation cell size is increased from a single pixel to the whole field-of-view. Table 3.1 summarizes the results where the standard deviation is calculated for each calibration temperature with 95% confidence

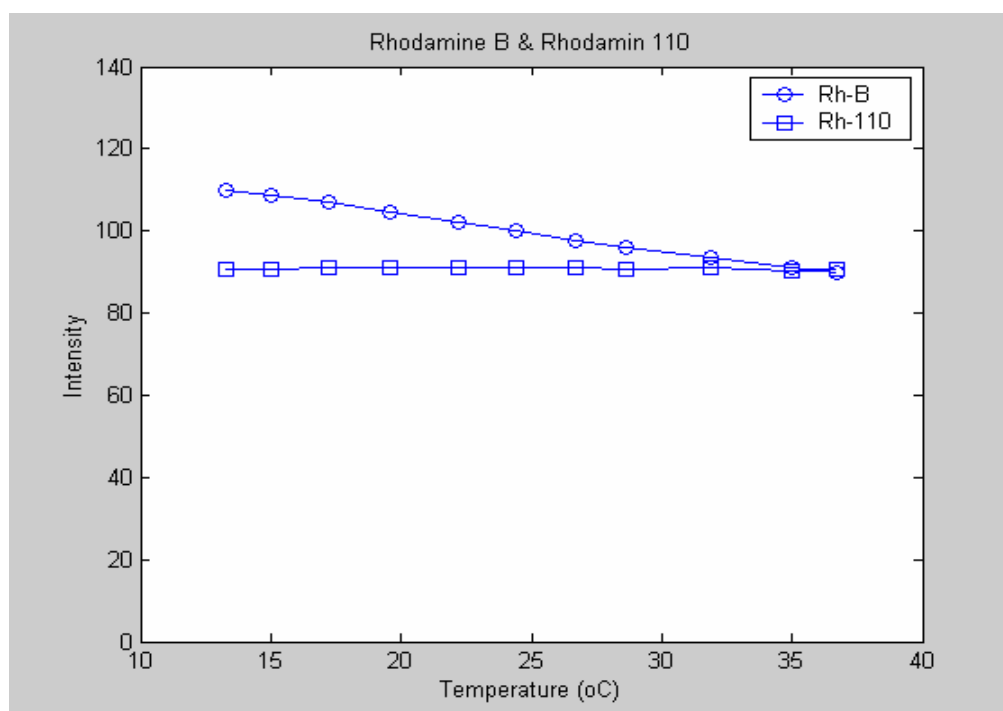


Fig. 3.3 Pixel Averaged Intensity of Rh-B and RH-110 Emission vs Temperature

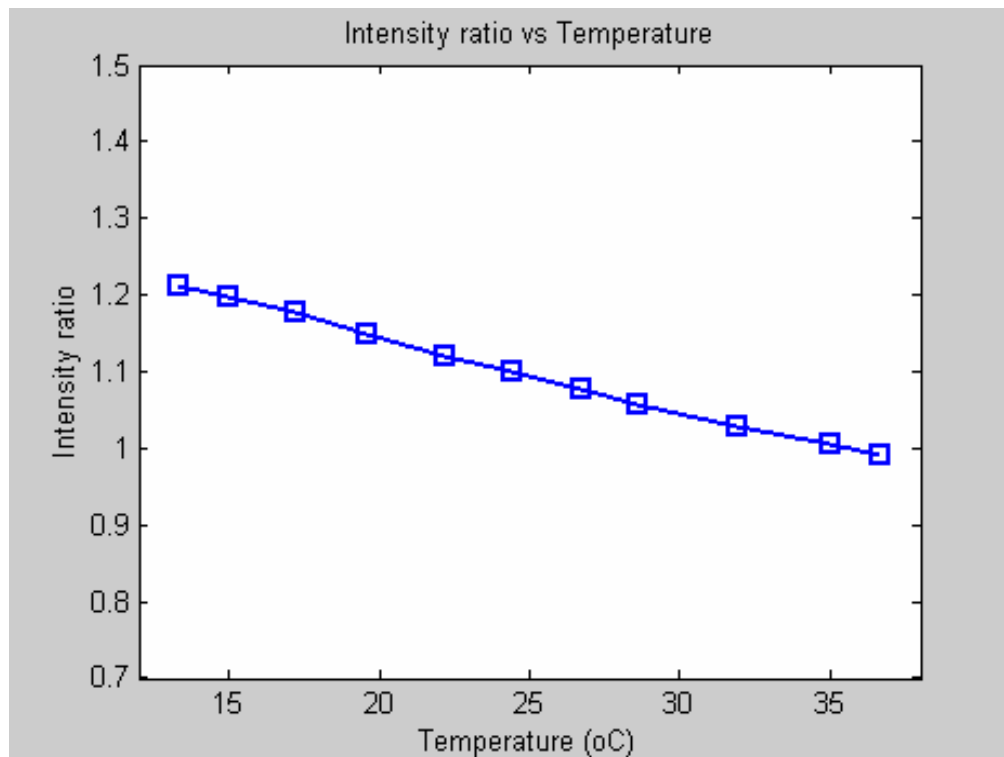
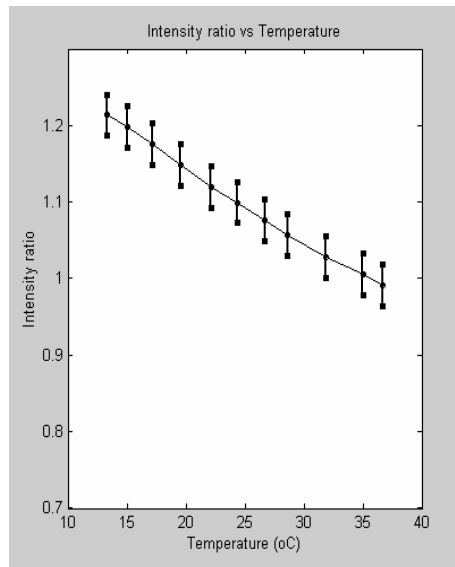


Fig. 3.4 Intensity Ratio vs Temperature

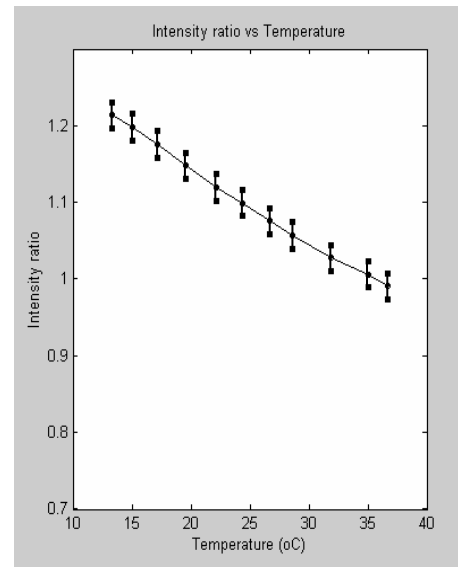
Table 3.1 Spatial Resolution and Corresponding Temperature Deviation for Calibration Data

Interrogation window Dimension (pixels)	Spatial Resolution (micron)	Intensity ratio deviation	Temperature deviation (°C)
1 x 1	12.5 x 12.5	±0.027	±3.270
4 x 4	50 x 50	±0.017	±2.055
8 x 8	100 x 100	±0.015	±1.813
64 x 48	800 x 600	±0.014	±1.692
320 x 240	4000 x 3000	±0.009	±1.087
320 x 480	4000 x 6000	±0.004	±0.483

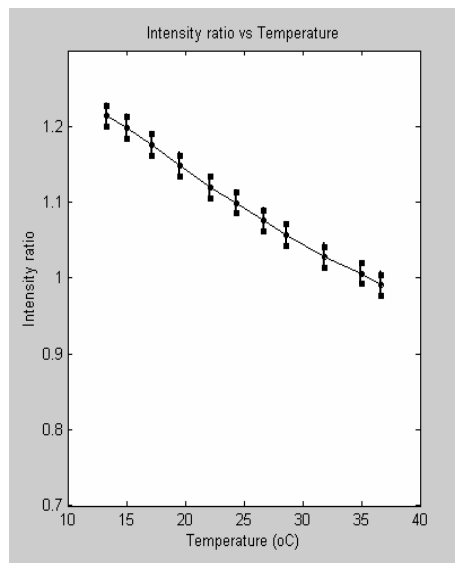
interval for a given interrogation cell size and listed deviations are the average values for the tested temperature range from 13 to 38 °C. The intensity ratio deviations are presented in the third column and the corresponding temperature deviations are shown in the fourth column. As the interrogating window dimension increase, the variation of intensity ratio decreases and diminishes ultimately to zero when the whole field-of-view



(a) 1 x 1 (12.5µm x 12.5µm)



(b) 8 x 8 (100µm x 100µm)



(c) 64 x 48 (800µm x 600µm)

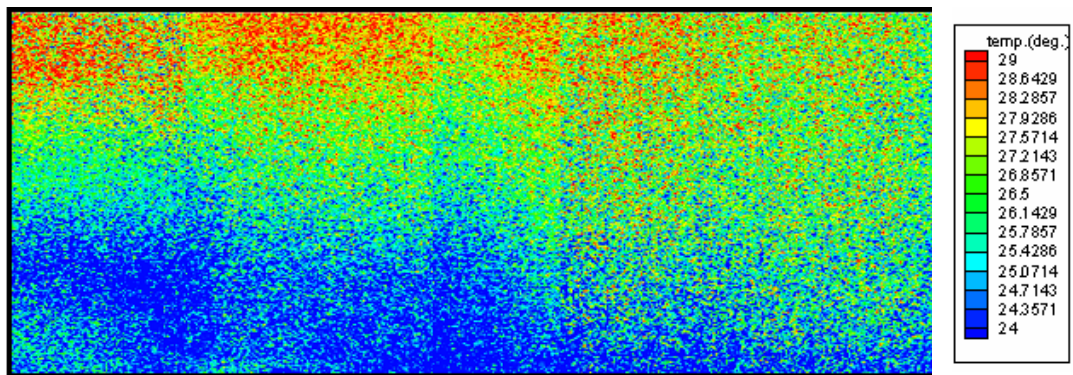
Fig. 3.5 Intensity Ratio vs Temperature: Derivation of Intensity with Interrogation Window Size

is considered as a single interrogation window. The corresponding pixel-to-pixel temperature variation (Table 3.1) is estimated as ± 3.27 K for 1 by 1 pixel, approximately ± 1.81 ° K for 8 by 8 pixels, and ± 1.69 K for 64 by 48 pixels. While the standard variations of intensity ratios, for a given temperature, persistently decrease with increasing window dimensions, note that the average intensity ratio remains constant for a given temperature regardless of the spatial resolution (Fig. 3.5).

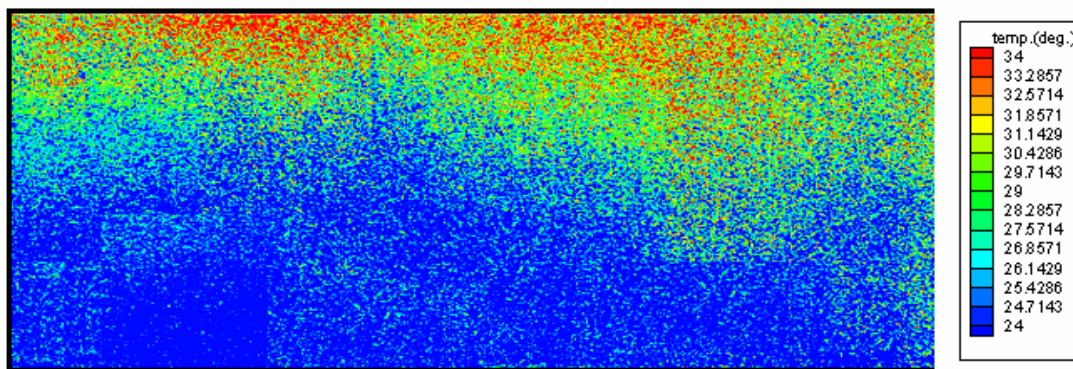
3.2 TEMPERATURE MEASUREMENT FOR THERMALLY STRATIFIED FIELDS

For a thermally stratified region in a parallel channel with the top surface heated and the bottom surface cooled, a linear temperature distribution is expected for the fluid between the two surfaces. The linear temperature profile will remain stationary if the boundary temperature conditions are persistent and heat loss through side surfaces is negligible. Using the ratiometric LIF thermometry, temperature profiles have been mapped for thermally stratified regions under steady temperature differential. Measurement accuracy and spatial resolution have been examined for the 10mm path parallel channels. The same cuvette (10mm x 10mm x 45mm) used for the calibration serves for the 10-mm parallel channel.

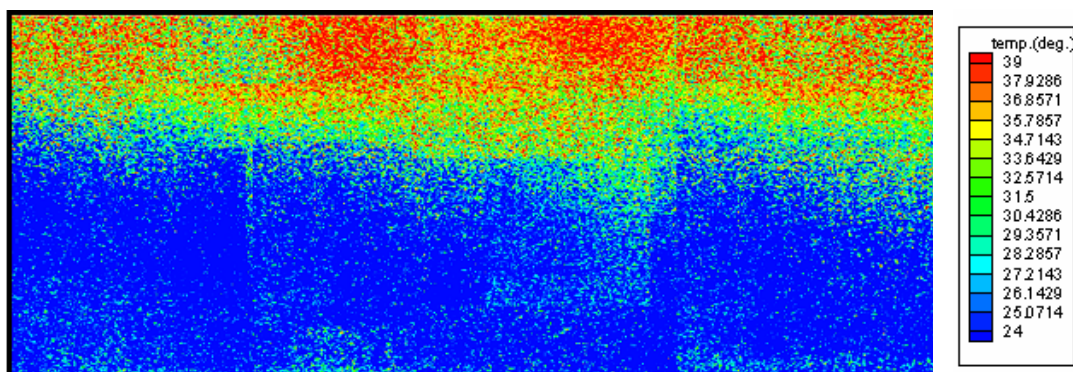
The same setup for calibration process (Fig 3.2) used with different thermbaths temperature setup and established thermally stratified field. To ensure more homogeneous thermal contact, the copper plate and the cuvette glass surface bonded by thermal grease. two thermocouple probes are embedded each upper and lower sides between copper plate and cuvette outer wall surface. The temperature reading is



(a) 24°C-29 °C



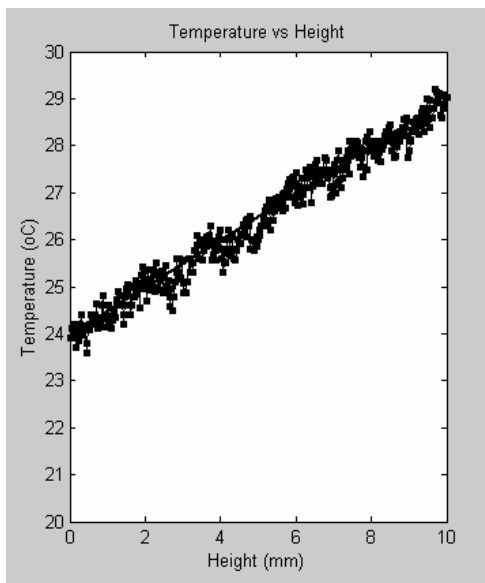
(b) 24°C-34 °C



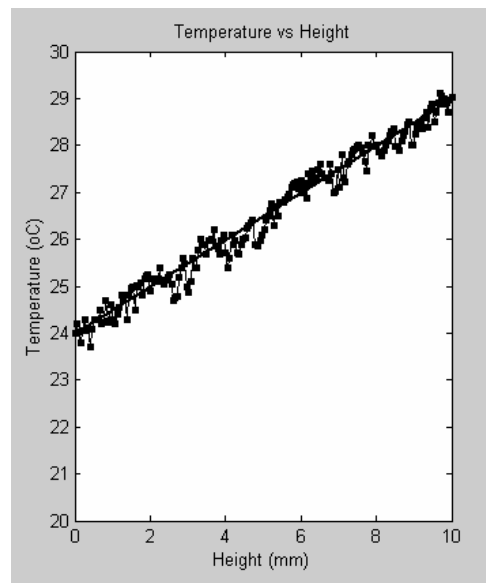
(c) 24°C-39 °C

Fig. 3.6 Thermally Stratified Fields under Three Different Conditions

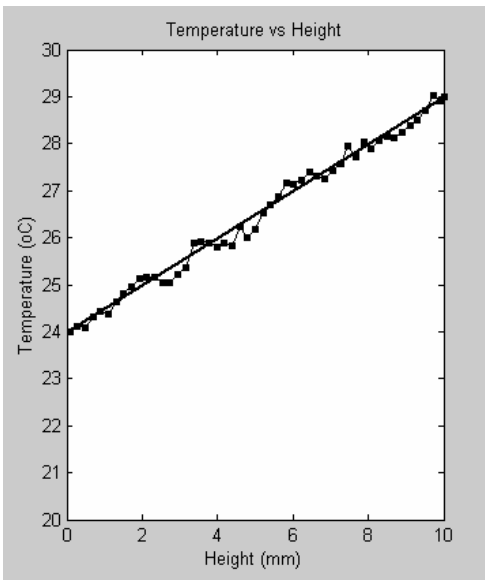
continuously sensed. To ensure steady state, waited for approximately 1-2 hours until its reading is not fluctuating. Fig. 3.6 show the thermally stratified characteristics inside the 0-mm channel as qualitatively and quantitatively. The LIF



**(a) Line-averaged 1x1 pixel
(23 μ m x 23 μ m)**



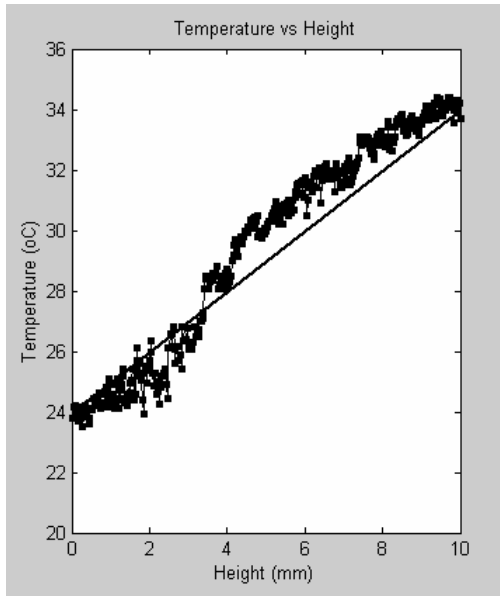
**(b) Line-averaged 2x2 pixels
(46 μ m x 46 μ m)**



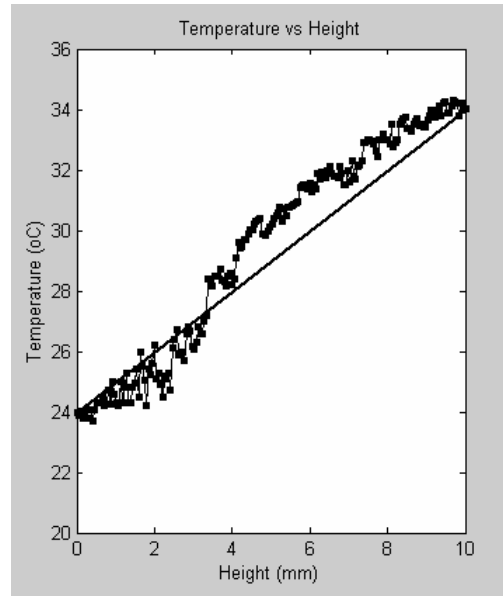
**(c) Line-averaged 8x8 pixels
(184 μ m x 184 μ m)**

Fig. 3.7 Line-averaged Measurement Result with Linear Prediction for Top 29°C and Bottom 24°C. (a) for 23 μ m x 23 μ m, (b) for 46 μ m x 46 μ m and (c) for 184 μ m x 184 μ m Interrogation Window Size

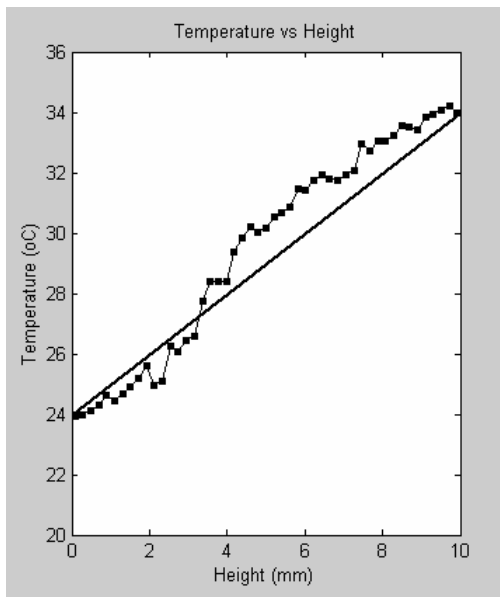
results, without any parametric adjustment, imposed specification, or often-misleading normalization between experimental data and predictions (Fig. 3.7, Fig. 3.8 and Fig. 3.9), show fairly impressive agreement with the ideal solution of linear profiles for all of the



**(a) Line-averaged 1x1 pixel
(23 μm x 23 μm)**

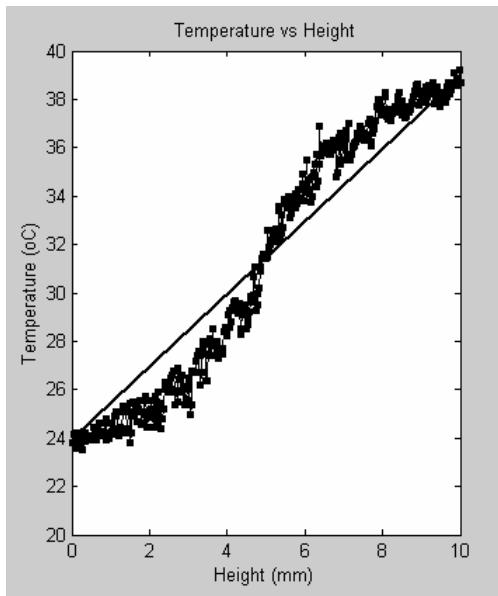


**(b) Line-averaged 2x2 pixels
(46 μm x 46 μm)**

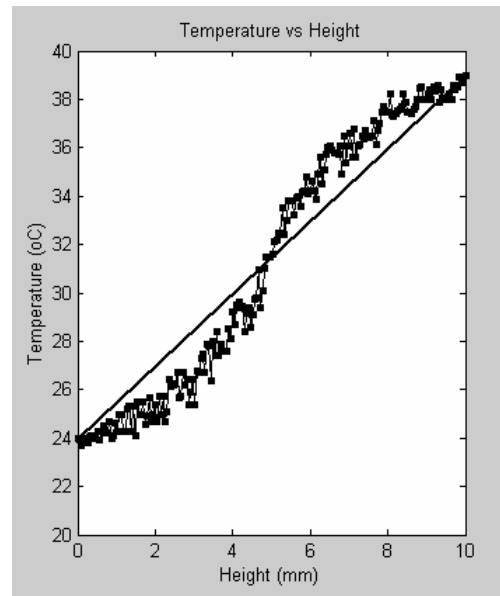


**(c) Line-averaged 8x8 pixels
(184 μm x 184 μm)**

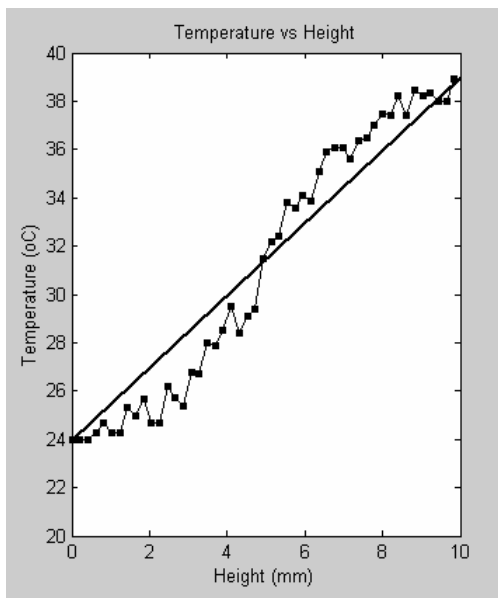
Fig. 3.8 Line-averaged Measurement Result with Linear Prediction for Top 34°C and Bottom 24°C. (a) for 23 μm x 23 μm , (b) for 46 μm x 46 μm and (c) for 184 μm x 184 μm Interrogation Window Size



(a) Line-averaged 1x1 pixel
(23 μ m x 23 μ m)



(b) Line-averaged 2x2 pixels
(46 μ m x 46 μ m)



(c) Line-averaged 8x8 pixels
(184 μ m x 184 μ m)

Fig. 3.9 Line-averaged Measurement Result with Linear Prediction for Top 39°C and Bottom 24°C. (a) for 23 μ m x 23 μ m, (b) for 46 μ m x 46 μ m and (c) for 184 μ m x 184 μ m Interrogation Window Size

tested cases.

Table 3.2 shows derivation of linear prediction with interrogation window size. As interrogation window size increase error is reduced by spatial resolution increase. And as the temperature differential increase the temperature fluctuation from the linear prediction increased.

Table 3.2 Standard Derivation of Temperature for Linear Prediction with Interrogation Window Size

Interrogation window size	24°C-29°C	24°C-34°C	24°C-39°C
1 by 1 (23µm x 23µm)	±0.22 K	±0.89 K	±1.29 K
2 by 2 (46µm x 46µm)	±0.19 K	±0.87 K	±1.28 K
8 by 8 (186µm x 186µm)	±0.12 K	±0.83 K	±1.20 K

3.3 TEMPERATURE MEASUREMENT FOR NATURAL CONVECTION FIELDS

The same setup with previous experiment, only temperature setting is changed as top surface is cold and bottom surface is hot to generate natural convection flows. The Rayleigh number is high enough to Buoyancy forces can overcome the resistance imposed by viscous forces ($\gg 1708$). Fig. 3.10 shows the results from ratiometric LIF

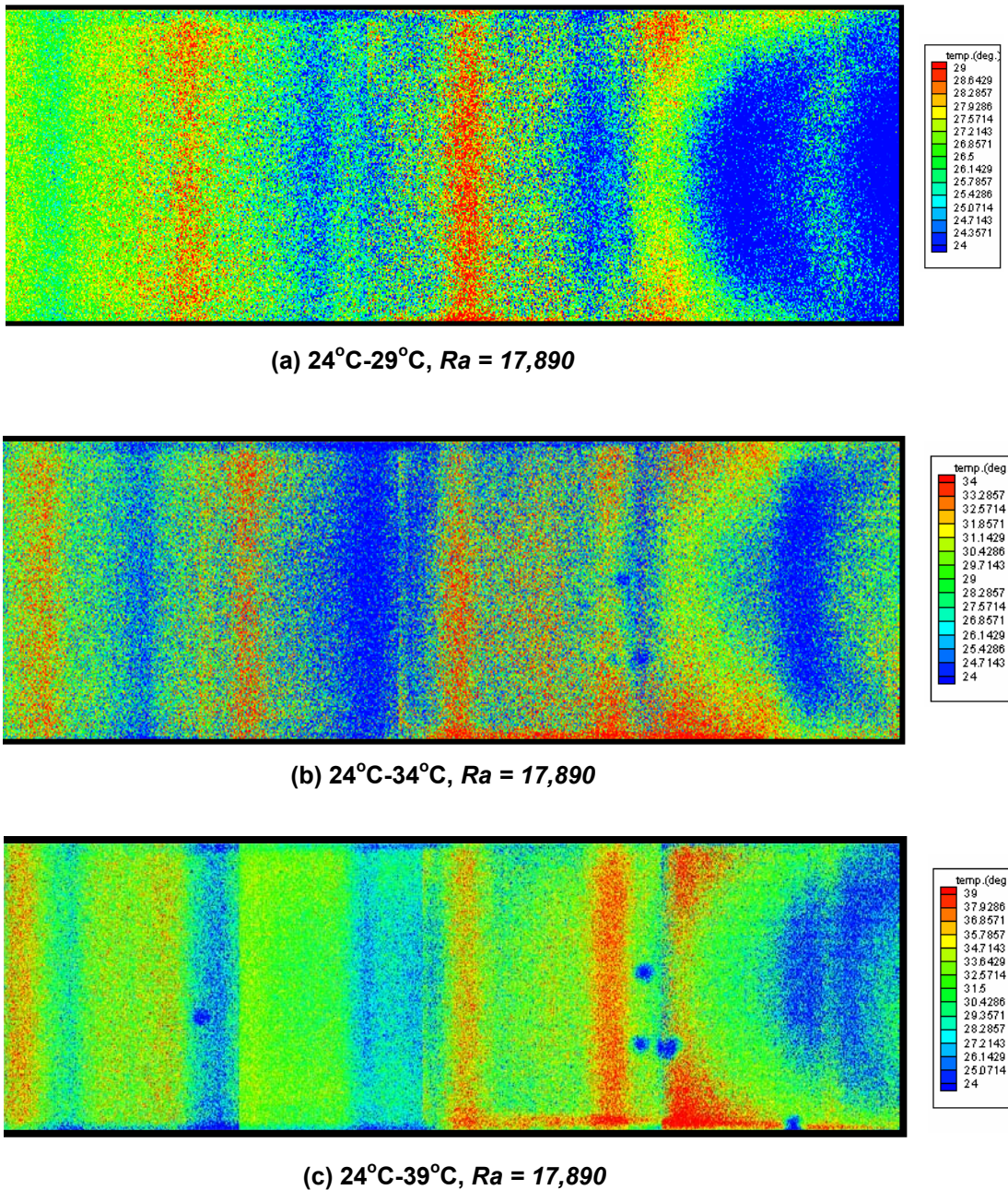


Fig. 3.10 Natural Convection Flows with Three Different Conditions. (a) Top 24°C and Bottom 29°C (b) Top 24°C and Bottom 34°C and (c) Top 24°C and Bottom 39°C.

thermometry, the red regions represent ascending flows with higher temperatures and the blue regions represent descending flows with lower temperatures. The green region,

which is wrapped by the red and blue regions, is the mixing area of natural convection flows. The right part of the test cuvette is under convection condition, with the air at room temperature of 24°C, because the laser is coming from the right side and should be open for laser illumination. The other side of the test section was well insulated except the front side for recording images.

CHAPTER IV

DISCUSSION

4.1 DIFFICULTIES FOR TEMPERATURE MEASUREMENT FOR HEATED EVAPORATING MENISCUS

In this chapter, I would like to discuss about the difficulties of temperature measurement for region of the heated evaporating meniscus. In this region, there is internal reflection of incident light and it causes re-absorption, which specially effect to the intensity of Rhodamine 110. Because the absorption and emission wavelength of Rhodamine 110 are relatively close to incident light wavelength rather than that of Rhodamine B (Fig.2.3). It increase Rhodamine 110 emission intensity without affecting to Rhodamine B emission intensity. As you can see Fig. 3.3, the emission intensity of Rhodamine B is always higher than that of Rhodamine 110 between 13°C and 39°C. However, in meniscus region it shows reversed tendency of intensity that Rhodamine 110 intensity is higher.

For this experiment, I designed the setup with 4mm of inner diameter glass pore with coiled heater and two thermocouple probes (Fig. 4.1). Fig 4.2 is the raw images of Rhodamine B and Rhodamine 110 emission under room temperature of 21.6°C. It shows that Rhodamine 110 emission is brighter than Rhodamine B emission.

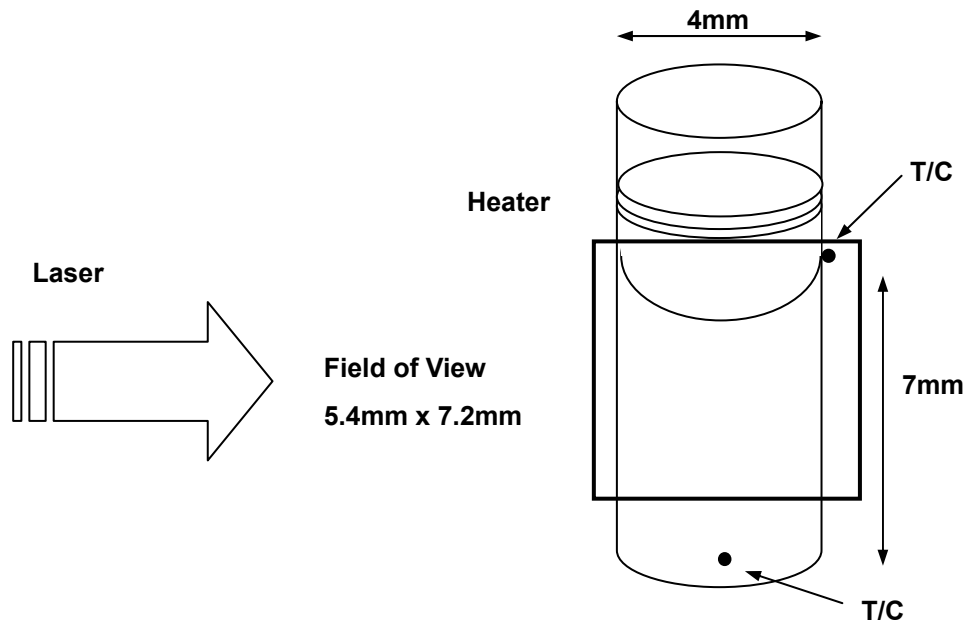


Fig. 4.1 Test Section for Heated Evaporating Meniscus

The mapping of temperature field with previous calibration data shows unreasonable results (Fig 4.3). Fig. 4.2 shows temperature gradient even under constant temperature as 21.6°C and quantitatively does not match with T/C's reading. This intensity bias coming from geometric shape of test section, the curvature. Under reflection condition, re-absorption by different index of reflection and direct CCD detection caused by filter leakage result intensity bias. Fig. 4.4 shows additional intensity term for Rhodamine 110. There are also error terms for Rhodamine B, however they are negligible compare to Rhodamine 110.

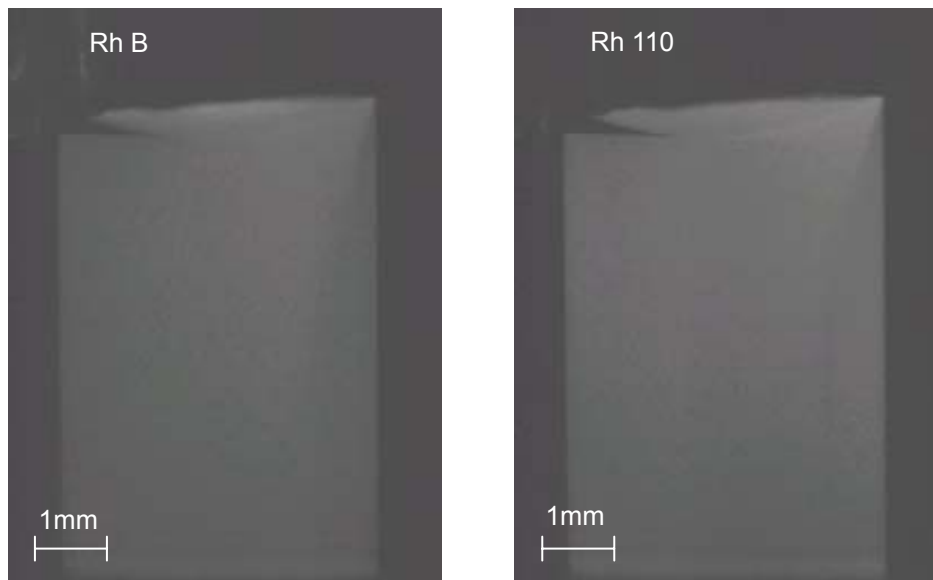


Fig 4.2 Raw Images of Meniscus at 21.6°C: Rhodamine 110 Intensity is Relatively Higher Than Rhodamine B Intensity (Rhodamine 110 Image is Brighter Than Rhodamine B Image)

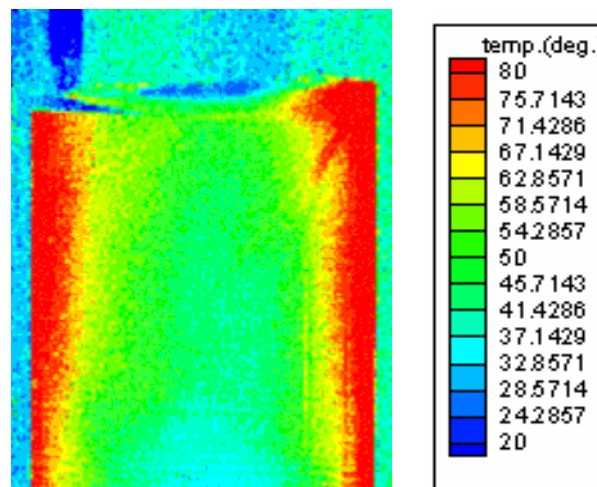


Fig. 4.3 Ratiometric LIF Result with Previous Calibration Data at Meniscus Region

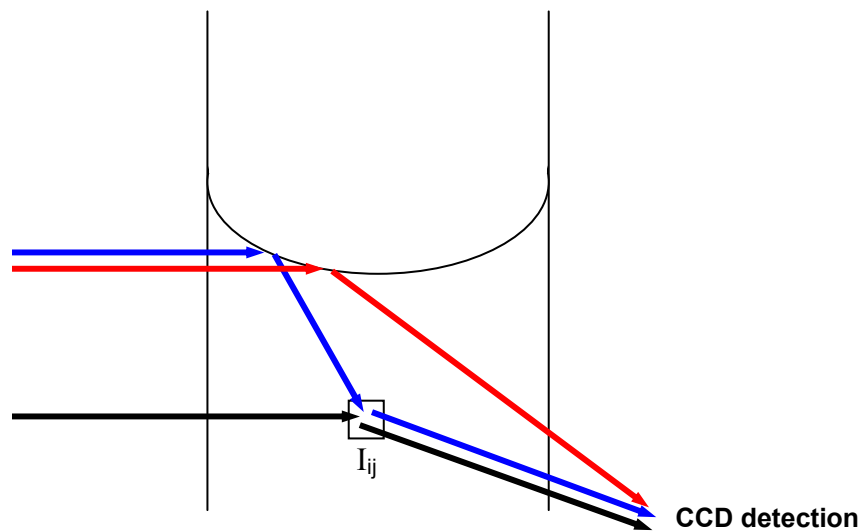
4.2 SUGGESTION OF A REMEDY FOR INTENSITY BIAS

Second calibration with known temperature condition accomplished. The error term express as equation. (4.1)

$$I_{ij} = I_{Fluorescence} + I_{re-absorption} + I_{direct\ detection} \quad (4.1)$$

The subscript ij means i th column j th row pixel. I_{ij} is the ratio of intensity detected to CCD. $I_{fluorescence}$ is represent fluorescence emission intensity without reflection. $I_{re-absorption}$ and $I_{direct\ detection}$ represent each error terms occurred under reflection condition.

To apply previous calibration data, I performed the second calibration. First, left the test section at the room temperature enough to reach steady state. Then take the



$$I_{ij} = I_{fluorescence} + I_{re-absorption} + I_{direct\ detection}$$

Fig. 4.4 Error Terms Coming from Internal Reflection: Re-absorption and Direct Detection

picture to get each images from Rhodamine 110 and Rhodamine B. Equation (4.1) can be rewrite to equation (4.2)

$$I_{ij} = I_{Fluorescence} + \alpha \quad (4.2)$$

At known temperature, we can determine $I_{Fluorescence}$ from previous calibration data. I_{ij} is the measured intensity ratio at known temperature. Then we can determine α , compensation factor, for every pixel for whole field of view. This α is mostly coming from Rhodamine 110, we can say it is independent on temperature change. Now, heat the test section, wait until steady state and take another images from each Rhodamine B and Rhodamine 110 emission. With these images rationing pixel by pixel and get $I_{ij, heating}$ for each pixel. The compensated $I_{Fluorescence}$, express to equation (4.3)

$$I_{Fluorescence} = I_{ij, heating} - \alpha \quad (4.3)$$

Now, apply the previous calibration data, we can obtain compensated values for temperature. Fig 4.5 is the compensated result with second calibration. Fig. 4.5 shows the temperature filed for top 38°C and bottom 22.5°C (Fig. 4.1), steady state. Though temperature range is reasonable to T/C's reading values, the temperature distribution shows still unreasonable result.

Lens effect also has a possibility to bias intensity (Fig 4.6 (a)). If I plot only the compensation factor, α , we can see lens effect like phenomena (Fig 4.6). I suggest that

consider lens effect and second calibration as a remedy for intensity bias at reflection condition. It can be correct by numerical method

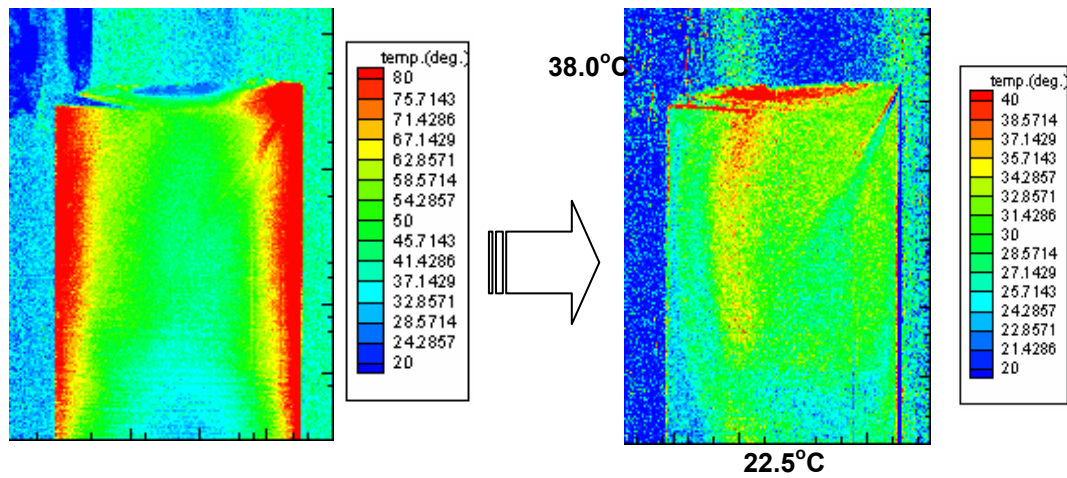


Fig. 4.5 Results after Second Calibration the Top T/C Reading is 38°C and Bottom T/C Reading is 22.5°C

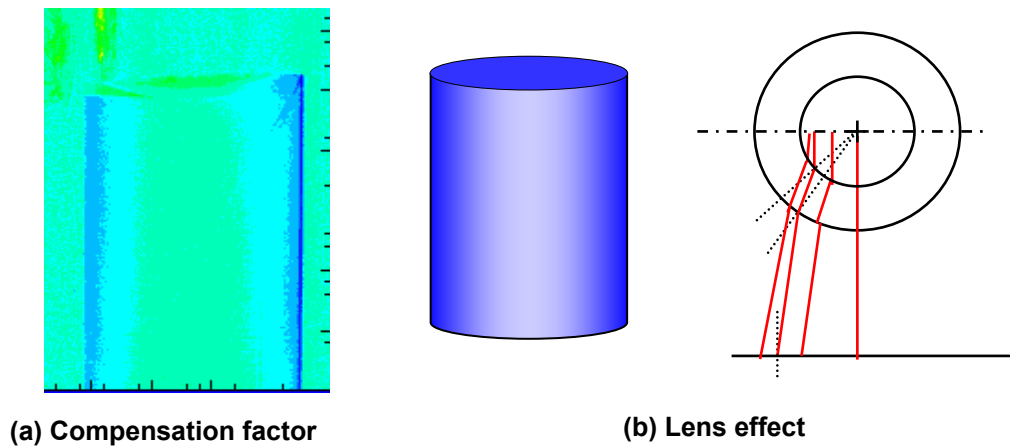


Fig.4. 6 Compensation Factor (a) and Lens Effect (b)

CHAPTER V

CONCLUSION

Ratiometric Laser Induced Fluorescence Thermometry applied to micro-scale temperature measurement for natural convection flow. The calibration data shows that $\pm 3.27^{\circ}\text{C}$ uncertainty for $12.5\mu\text{m}$ by $12.5\mu\text{m}$ and $\pm 1.8^{\circ}\text{C}$ uncertainty for $100\mu\text{m}$ by $100\mu\text{m}$ interrogation window size. For thermally stratified field, the linear prediction matched within $\pm 1.3^{\circ}\text{C}$ for $23\mu\text{m}$ by $23\mu\text{m}$ interrogation window size. For the natural convection flows, the isothermal contour lines were observed with micro-scale resolution.

For heated evaporating meniscus region, several difficulties to apply ratiometric LIF thermometry are identified and second calibration was considered.

In this study, the ratiometric Laser Induced Fluorescence (LIF) thermometry applied to measure temperature in micro-scale resolution and confirmed with natural convection flows. Potential difficulties for applying this technique to evaporating thin film region are identified.

CHAPTER VI

RECOMMENDATIONS FOR FUTURE STUDY

To obtain more accurate, smaller spatial resolution, I recommend using intensified CCD with high magnification lens. To apply this technique, the calibration process is most important part in experiment. Clean optics also can determine quality of the calibration data. For doing the experiment, insulation is very important to measure accurate temperature, because the fluorescence emission is very sensitive to temperature change.

For the meniscus region, illumination direction and reflection phenomena is major problem to make intensity bias, to overcome this problem, I recommend to use narrow bandwidth filters for blocking direct detection along with second calibration. If the test section has circular shape, do not exclude lens effect.

REFERENCES

- [1] Park, J. S., Kihm, K. D. and Pratt, D. M., 2000, “Molecular Tagging Fluorescence Velocimetry (MTFV) to Lagrangian Flow Field Mapping inside Evaporating Meniscus: Potential use for Micro-scale Applications, *Journal of Flow Visualization & Image Processing*. Vol 8, pp 177-187
- [2] Coolen, M. C. J., Kieft, R. N., Rindt, C. C. M., and van Steenhoven, A. A., 1999, “Application of 2-D LIF Temperature Measurements in Water Using a Nd-Yag Laser,” *Experiments in Fluids*, **27**, pp. 420-426.
- [3] Sakakibara, J. and Adrian, R. J., 1997, “Measurement of Whole Field Temperature Using Two-Color LIF,” *J. Visualization Soc., Japan* 17:333-336.
- [4] Sakakibara, J. and Adrian, R. J., 1999, “Whole Field Measurement of Temperature in Water Using Two-Color Laser Induced Fluorescence,” *Experiments in Fluids*, **26**, pp. 7-15.
- [5] Kim, H. J. and Kihm, K. D., 2001 “Application of a Two-Color Laser Induced Fluorescence(LIF) Technique for Temperature Mapping”, *Proc. of 2001 ASME International Mechanical Engineering Congress and Exposition*, New York, 221-227, November
- [6] Renk, F. J. and Wayner, P. C., Jr., 1979, “An Evaporating Ethanol Meniscus: Part 1, Experimental studies”, *ASME Journal of Heat Transfer*, **101**, No. 1, pp. 55-58
- [7] Renk, F. J. and Wayner, P. C., Jr., 1979, “An evaporating Ethanol Meniscus: Part 2, Analytical studies”, *ASME Journal of Heat Transfer*, **101**, No. 1, pp. 59-62

- [8] Herman, B., 1998, *Fluorescence Microscopy*, Second Edition, Springer, Berlin.
- [9] Andrews, D. L., 1986, *Lasers in Chemistry*, Springer-Verlag, Berlin.

VITA

HEON JU LEE

Mechanical Engineering Department

Texas A&M University

College Station, TX 77843-3123

Phone: (979) 845-6188

E-mail: lee_heon_ju@hotmail.com

Personal Data

Date of Birth: May 6, 1977

Parents: Chun Sik Lee, Chung Cha Kim

Permanent Address: 10-702 Woosung il-cha Apt., Dae-Chi-Dong,
Kangnam-Gu, Seoul, Korea

Education

M.S. Mechanical Engineering, Texas A&M University, Aug. 2003

B.S. Mechanical Engineering, Korea University, Feb. 2001

Professional Experience

09/02-05/03 Research Assistant in the Department of Mechanical
Engineering, Texas A&M University, College Station

09/01-08/02 Teaching Assistant in the Department of Mechanical
Engineering, Texas A&M University, College Station

08/99-08/01 Research Assistant in Thermal/Flow Control Center,
Korea Institute of Science and Technology, Seoul, Korea